Supplement of Atmos. Chem. Phys., 15, 5773–5801, 2015
http://www.atmos-chem-phys.net/15/5773/2015/
doi:10.5194/acp-15-5773-2015-supplement

Atmospheric Chemistry and Physics
Open Access

Supplement of

Modeling the formation and aging of secondary organic aerosols in Los Angeles during CalNex 2010

P. L. Hayes et al.

Correspondence to:

Table SI-1. The VOC parameters used to model the formation of SOA (Atkinson and Arey, 2003; Carter, 2010; Tsimpidi et al., 2010). All aging of VOCs after the initial oxidation reaction occurs with a gas-phase rate constant of $k_{OH} = 1 \times 10^{-11}$ cm^3 $molec^{-1}$ s^{-1}. Note that the aging rate constant was erroneously reported as 4×10^{-11} cm^3 $molec^{-1}$ s^{-1} in Tsimpidi et al. All SOA from VOCs has a ΔH_{vap} of 36 kJ mol^{-1} (Volkamer et al., 2006).

Precursor Family Name	Compounds	k_{OH} (cm^3 $molec^{-1}$ s^{-1})	ΔVOC/ΔCO (ppt ppb^{-1})	Stoichiometric SOA yield High-NO_X, 298 K, (μg m^{-3})				M.W. (g mol^{-1})
				1	10	100	1000	
ALK5	Methylcyclopentane	5.68×10^{-12}	0.566	0.000	0.015	0.000	0.000	150
	Cyclohexane	6.97×10^{-12}	0.285					
	Methylcyclohexane	9.64×10^{-12}	0.202					
	n-Heptane	6.76×10^{-12}	0.398					
	2-Methyl Hexane	6.89×10^{-12}	0.385					
	3-Methyl Hexane	7.17×10^{-12}	0.460					
	2,3-Dimethyl Pentane	7.15×10^{-12}	0.252					
	2,4-Dimethyl Pentane	4.77×10^{-12}	0.171					
	2,2,3-Trimethyl Butane	3.81×10^{-12}	0.031					
	N-Octane	8.11×10^{-12}	0.197					
	3-Methyl Heptane	8.59×10^{-12}	0.131					
	2-Methyl Heptane	8.31×10^{-12}	0.171					
	2,2,4-Trimethyl Pentane	3.34×10^{-12}	0.476					
	2,3,4-Trimethyl Pentane	6.60×10^{-12}	0.171					
	2,3,3-Trimethyl Pentane	4.40×10^{-12}	0.194					
	N-Nonane	9.70×10^{-12}	0.220					
	N-Decane	11.0×10^{-12}	0.180					
	Undecane	12.3×10^{-12}	0.290					

Table SI-1 (continued).

Precursor Family Name	Compounds	k_{OH} (cm^3 $molec^{-1}$ s^{-1})	ΔVOC/ΔCO (ppt ppb^{-1})	Stoichiometric SOA yield High-NO_X, 298 K, (μg m^{-3})				Molecular Weight (g mol^{-1})
				1	10	100	1000	
OLE1	Propene	26.3×10^{-12}	3.740	0.001	0.005	0.038	0.150	120
	1-Butene	31.4×10^{-12}	0.340					
	1-Pentene	31.4×10^{-12}	0.112					
	2-methyl-1-butene	61.0×10^{-12}	0.250					
	3-methyl-1-butene	31.8×10^{-12}	0.058					
OLE2	1,3-Butadiene	66.6×10^{-12}	0.350	0.003	0.026	0.083	0.27	120
	trans-2-Pentene	67.0×10^{-12}	0.097					
	cis-2-Pentene	65.0×10^{-12}	0.050					
	Styrene	58.0×10^{-12}	0.220					
ARO1	Toluene	5.63×10^{-12}	3.180	0.003	0.165	0.300	0.435	150
	Ethylbenzene	7.00×10^{-12}	0.570					
	i-Propylbenzene	6.30×10^{-12}	0.030					
	n-Propylbenzene	5.80×10^{-12}	0.110					
	Benzene	1.22×10^{-12}	1.300					
ARO2	o-Ethyltoluene	9.57×10^{-12}	0.120	0.002	0.195	0.300	0.435	150
	1,2,3-Trimethylbenzene	11.9×10^{-12}	0.240					
	1,2,4-Trimethylbenzene	32.7×10^{-12}	0.620					
	1,3,5-Trimethylbenzene	32.5×10^{-12}	0.310					
	m-xylene	56.7×10^{-12}	1.790					
	p-xylene	23.1×10^{-12}	1.790					

Table SI-1 (continued).

Precursor Family Name	Compounds	k_{OH} (cm^3 $molec^{-1}$ s^{-1})	ΔVOC/ΔCO (ppt ppb^{-1})	Stoichiometric SOA yield High-NO_X, 298 K, (μg m^{-3})				Molecular Weight (g mol^{-1})
				1	10	100	1000	
NAPH	Naphthalene	24.4×10^{-12}	0.065	0.165	0.005	0.516	0.881	150
	1-Methylnaphthalene	40.9×10^{-12}	0.01					
	2-Methylnaphthalene	48.6×10^{-12}	0.021					
ISOP	Isoprene (Anthropogenic)	100×10^{-12}	N/A (see text)	0.001	0.023	0.015	0.000	136
	Isoprene (Biogenic)	100×10^{-12}	N/A (see text)					
TERP	α-Pinene + β-Pinene + Limonene	98.2×10^{-12}	N/A (see text)	0.012	0.122	0.201	0.5	180

Table SI-2. Summary of the Robinson et al. (2007) and the Grieshop et al. (2009) parameterizations for P-S/IVOCs.

***c** @ 300 K (μg m^{-3})**	***ΔH$_{vap}$* (kJ mol^{-1})**		**Molecular Weight (g mol^{-1})**		**Fraction of total P-S/IVOC (%)**
ROB & GRI	ROB	GRI	ROB	GRI	ROB & GRI
0.01	112	77	250	524	1.2
0.1	106	73	250	479	2.4
1	100	69	250	434	3.6
10	94	65	250	389	5.6
100	88	61	250	344	7.2
1,000	82	57	250	299	12
10,000	76	54	250	254	16
100,000	70	50	250	208	20
1,000,000	64	46	250	163	32

	ROB	**GRI**
k_{OH} at 300 K (cm^3 molec^{-1} s^{-1})	4×10^{-11}	2×10^{-11}
Oxygen gain per oxidation generation (%)	7.5	40
Volatility bin decrease per oxidation generation	1 order of magnitude	2 orders of magnitude

Table SI-3. Initial concentrations of primary IVOCs predicted by the box model (ROB parameterization) in comparison with data from Zhao et al. (2014) as a function of the saturation concentration (C*) at 298 K. Note that the corresponding results for the GRI parameterization are very similar with the concentration being 8% higher due to differences in the ΔH_{vap}.

C* (μg m^{-3})	**Estimated Primary IVOCs (μg m^{-3})**	**Estimated Primary IVOCs without cooking emissions (μg m^{-3})**	**Measured Primary IVOCs (μg m^{-3})**
10^3	2.47	1.70	0.21 (± 0.07)
10^4	3.30	2.27	1.39 (± 0.29)
10^5	4.12	2.84	2.64 (± 0.64)
10^6	6.59	4.54	3.82 (± 0.99)

Table SI-4. Summary of tracers used by the EPA group to determine the concentration of SOA from a certain precursor.

Tracer Molecule	**Precursors**	**Reference**
2-Methylglyceric acid	Isoprene	Edney et al. *Atmos. Environ.* **2005,** 5281-5289.
2-Methylthreitol	Isoprene	Edney et al. *Atmos. Environ.* **2005,** 5281-5289.
2-Methylerythritol	Isoprene	Edney et al. *Atmos. Environ.* **2005,** 5281-5289.
3-Acetyl pentanedioic acid	Monoterpenes	Jaoui et al. *Environ. Sci. Technol.* **2005,** 5661-5673.
3-Acetyl hexanedioic acid	Monoterpenes	Jaoui et al. *Environ. Sci. Technol.* **2005,** 5661-5673.
3-Methyl-1,2,3-butanetricarboxylic acid	Monoterpenes	Szmigielski et al. *J. Geophys. Res.-Atmos.* **2007,** L24811.
3-Hydroxyglutaric acid	Monoterpenes	Claeys et al. *Environ. Sci. Technol.* **2005,** 1628-1634.
3-Hydroxy-4,4-dimethylglutaric acid	Monoterpenes	Claeys et al. *Environ. Sci. Technol.* **2005,** 1628-1634.
Pinic acid	Monoterpenes	Claeys et al. *Environ. Sci. Technol.* **2005,** 1628-1634.

Figure Captions

Figure SI-1. The evolution of OA/ΔCO versus photochemical age for CalNex separated by cloudy days and mostly clear days. ΔCO is calculated as the difference of the ambient CO and the background CO (105 ppb) (Hayes et al., 2013). The cloudy days are 17 and 27 May 2010, as well as 11 June 2010.

Figure SI-2. Model/measurement comparisons of the diurnal cycles for selected VOC mixing ratios as well as for POA mass concentrations. Note that for the VOCs the GRI+TSI, ROB+TSI, PYE+TSI, ROB+4xV model variations give the same results.

Figure SI-3. (Top) Scatter plots for naphthalene, 1-methylnaphthalene, and 2-methylnaphthalene versus CO mixing ratios. Data includes only measurements from 00:00 – 06:00 (local time) to minimize the impact of photochemical oxidation on the PAH concentrations. Also shown in the top panels are the linear ODR analyses of the data with the y-intercept fixed at 105 ppb CO, which is the background CO concentration (Hayes et al., 2013). For more information on the methodology used to measure naphthalene and the methylnaphthalenes see Presto et al. (2011; 2012). **(Bottom)** Model and measurement diurnal cycles for naphthalene, 1-methylnaphthalene, and 2-methylnaphthalene.

Figure SI-4. Anthropogenic CO fluxes on a 12 km grid in Southern California that are used in the WRF-Chem simulation. The box indicates the region around and inside LA where the emissions of atmospheric species are set to zero in order to determine the concentration of background SOA.

Figure SI-5. Model/measurement comparison of SOA mass concentrations after excluding from the model P-S/IVOC emissions, or in the case of the PYE+TSI variation, SVOC emissions from cooking-related activities. Otherwise the figure is identical to Figure 4 in the main text.

Figure SI-6: The estimated relative concentration of SOA from gasoline vehicles, diesel vehicles, cooking emissions, in-basin biogenic emissions, and the regional background.

Figure SI-7: Model/measurement comparison of SOA mass concentration after reducing the emission of IVOCs in the model by one-half. Otherwise the figure is identical to Figure 4 in the main text.

Figure SI-8: Scatter plots of **(A)** benzene, **(B)** low-yield aromatic VOCs, and **(C)** high-yield aromatic VOCs measured by GC-MS against the concentration predicted by WRF-CMAQ. The low-yield aromatics correspond to the family ARO1 and the high-yield aromatics to the family ARO2 in Table SI-1. Also shown for reference are the 5:1, 1:1, and 1:5 lines. **(D)** SOA/ΔCO as a function of photochemical age as determined by measurements (black circles) and predicted by WRF-CMAQ (red squares). The left and right axes are plotted on different scales for clarity. Photochemical age is determined from the ratio of NO_Y to NO_X (Hayes et al., 2013).

Figure SI-9: Time series of inorganic and organic aerosols at the Pasadena ground site during CalNex measured by an AMS or modeled by WRF-CMAQ. For SOA, the concentration was determined using positive matrix factorization analysis of the AMS measurements. The AMS measurements have a PM_1 size cut, and the WRF-CMAQ model results are the sum of the Aiken and accumulation modes, which corresponds to $PM_{2.5}$. (Note: In WRF-CMAQ all SOA species are assigned to the accumulation mode.)

Figure SI-10: Scatter plots of the inorganic aerosol measurements from an AMS against the modeled concentrations from WRF-CMAQ. The data shown are the same as in Figure SI-9. Also shown are the corresponding linear ODR analyses and corresponding fit parameters.

References

Atkinson, R. and Arey, J. (2003) Atmospheric degradation of volatile organic compounds. Chem. Rev. 103, 4605-4638.

Carter, W.P.L. (2010) Development of the SAPRC-07 chemical mechanism. Atmos. Environ. 44, 5324-5335.

Grieshop, A.P., Logue, J.M., Donahue, N.M. and Robinson, A.L. (2009) Laboratory investigation of photochemical oxidation of organic aerosol from wood fires 1: measurement and simulation of organic aerosol evolution. Atmos. Chem. Phys. 9, 1263-1277.

Hayes, P.L., Ortega, A.M., Cubison, M.J., Froyd, K.D., Zhao, Y., Cliff, S.S., Hu, W.W., Toohey, D.W., Flynn, J.H., Lefer, B.L., Grossberg, N., Alvarez, S., Rappenglück, B., Taylor, J.W., Allan, J.D., Holloway, J.S., Gilman, J.B., Kuster, W.C., de Gouw, J.A., Massoli, P., Zhang, X., Liu, J., Weber, R.J., Corrigan, A.L., Russell, L.M., Isaacman, G., Worton, D.R., Kreisberg, N.M., Goldstein, A.H., Thalman, R., Waxman, E.M., Volkamer, R., Lin, Y.H., Surratt, J.D., Kleindienst, T.E., Offenberg, J.H., Dusanter, S., Griffith, S., Stevens, P.S., Brioude, J., Angevine, W.M. and Jimenez, J.L. (2013) Organic aerosol composition and sources in Pasadena, California during the 2010 CalNex campaign. J. Geophys. Res.-Atmos., 9233-9257.

Presto, A.A., Hennigan, C.J., Nguyen, N.T. and Robinson, A.L. (2012) Determination of Volatility Distributions of Primary Organic Aerosol Emissions from Internal Combustion Engines Using Thermal Desorption Gas Chromatography Mass Spectrometry. Aerosol Sci. Technol. 46, 1129-1139.

Presto, A.A., Nguyen, N.T., Ranjan, M., Reeder, A.J., Lipsky, E.M., Hennigan, C.J., Miracolo, M.A., Riemer, D.D. and Robinson, A.L. (2011) Fine particle and organic vapor emissions from staged tests of an in-use aircraft engine. Atmos. Environ. 45, 3603-3612.

Robinson, A.L., Donahue, N.M., Shrivastava, M.K., Weitkamp, E.A., Sage, A.M., Grieshop, A.P., Lane, T.E., Pierce, J.R. and Pandis, S.N. (2007) Rethinking organic aerosols: Semivolatile emissions and photochemical aging. Science 315, 1259-1262.

Tsimpidi, A.P., Karydis, V.A., Zavala, M., Lei, W., Molina, L., Ulbrich, I.M., Jimenez, J.L. and Pandis, S.N. (2010) Evaluation of the volatility basis-set approach for the simulation of organic aerosol formation in the Mexico City metropolitan area. Atmos. Chem. Phys. 10, 525-546.

Volkamer, R., Jimenez, J.L., San Martini, F., Dzepina, K., Zhang, Q., Salcedo, D., Molina, L.T., Worsnop, D.R. and Molina, M.J. (2006) Secondary organic aerosol formation from anthropogenic air pollution: Rapid and higher than expected. Geophys. Res. Lett. 33, L17811.

Zhao, Y., Hennigan, C.J., May, A.A., Tkacik, D.S., de Gouw, J.A., Gilman, J.B., Kuster, W.C., Borbon, A. and Robinson, A.L. (2014) Intermediate-Volatility Organic Compounds: A Large Source of Secondary Organic Aerosol. Environ. Sci. Technol. 48, 13743-13750.

Figure SI-1

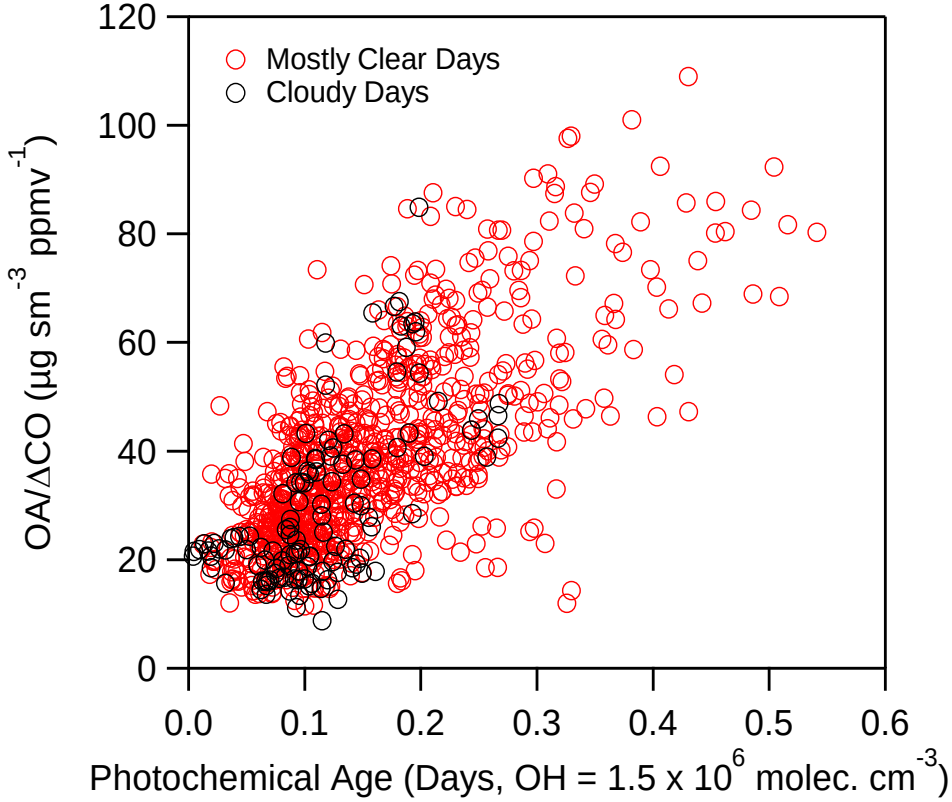
Mostly Clear Days
Cloudy Days
OA/ΔCO (μg sm^{-3} ppmv^{-1})
Photochemical Age (Days, OH = 1.5 x 10^{6} molec. cm^{-3})
0
20
40
60
80
100
120
0.0
0.1
0.2
0.3
0.4
0.5
0.6

Figure SI-2

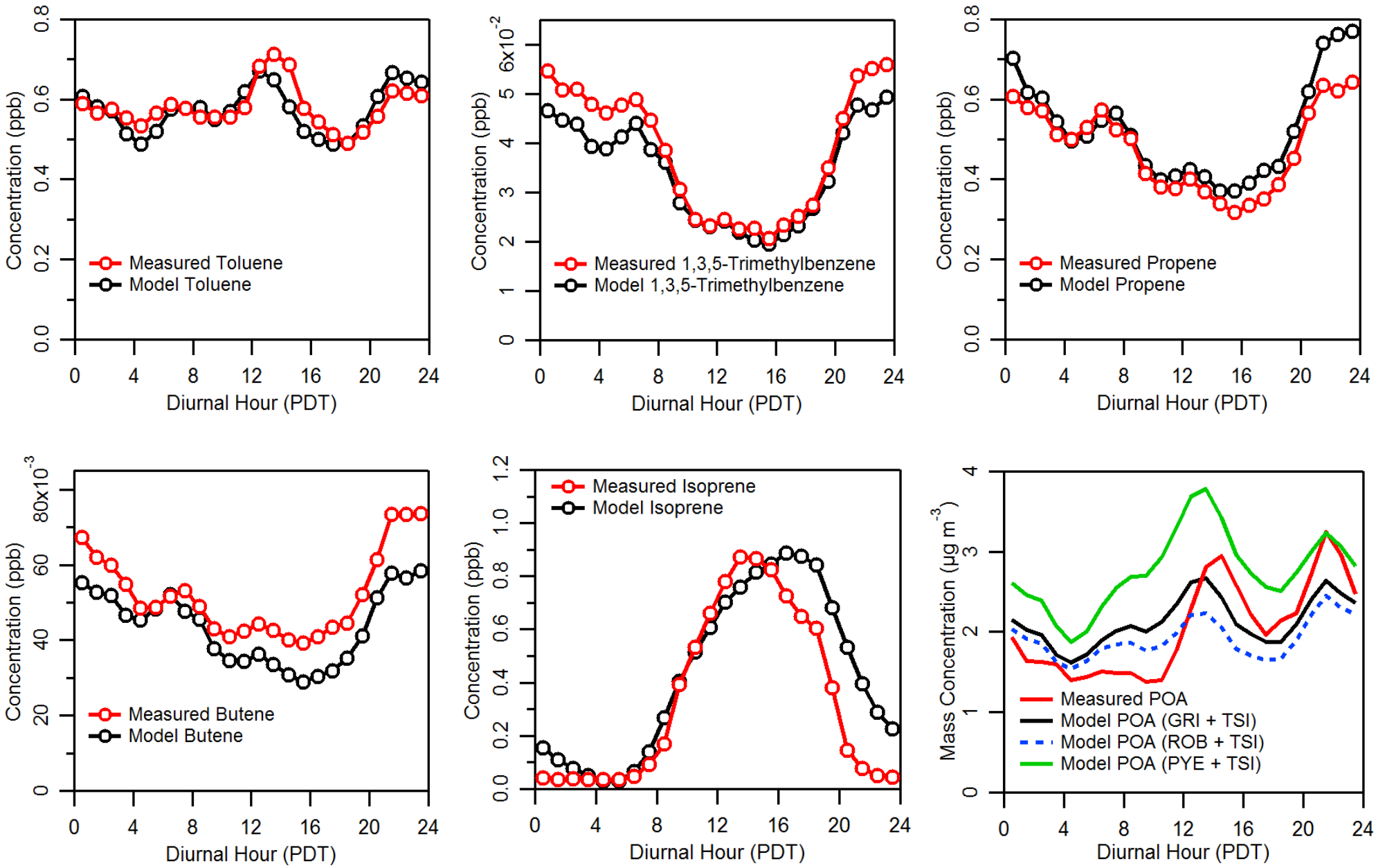
Concentration (ppb)
Diurnal Hour (PDT)
Measured Toluene
Model Toluene
Measured 1,3,5-Trimethylbenzene
Model 1,3,5-Trimethylbenzene
6x10^-2
Measured Propene
Model Propene
80x10^-3
Measured Butene
Model Butene
Measured Isoprene
Model Isoprene
Mass Concentration (µg m^-3)
Measured POA
Model POA (GRI + TSI)
Model POA (ROB + TSI)
Model POA (PYE + TSI)

Figure SI-3

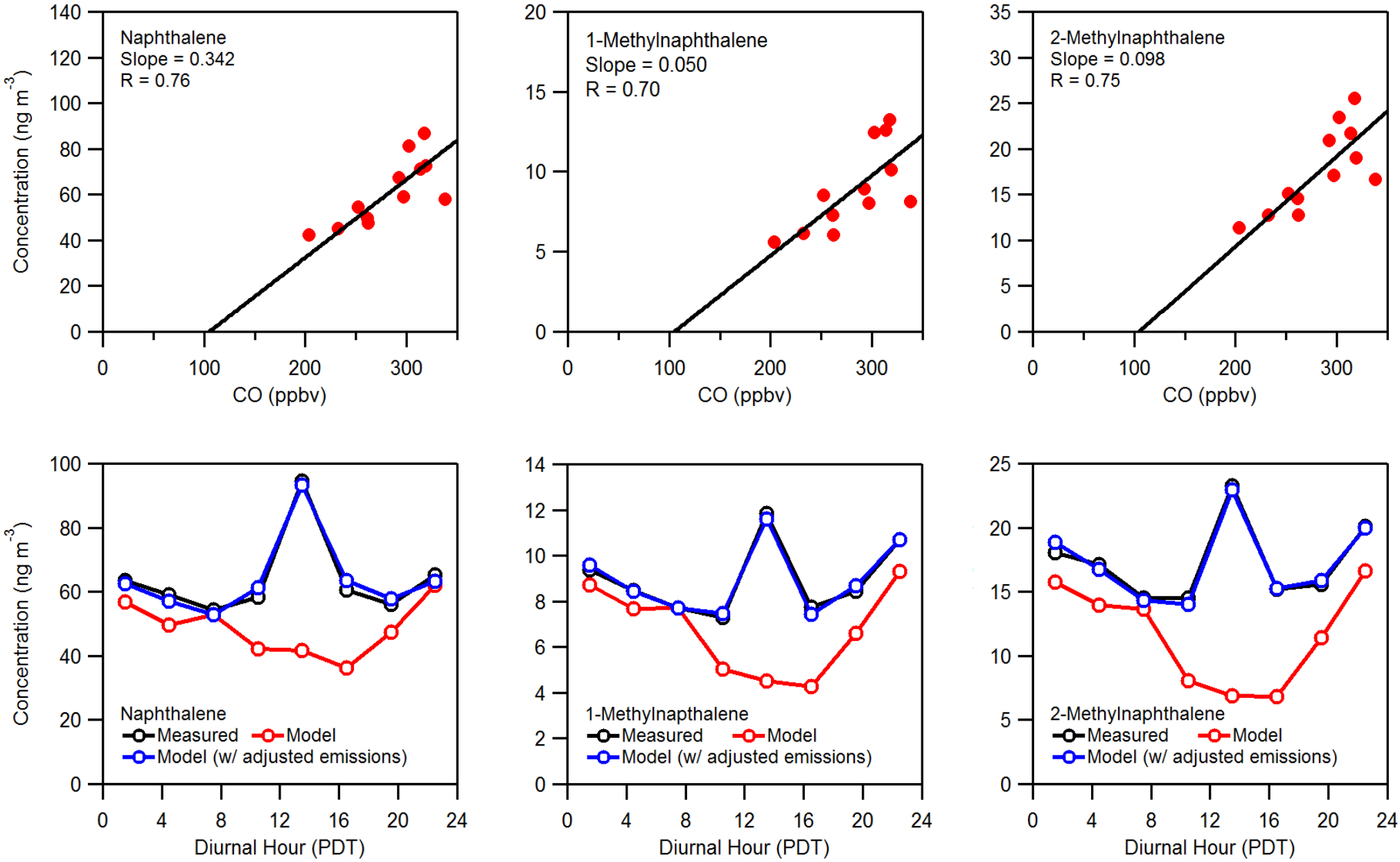
Naphthalene
Slope = 0.342
R = 0.76
1-Methylnaphthalene
Slope = 0.050
R = 0.70
2-Methylnaphthalene
Slope = 0.098
R = 0.75
Concentration (ng m-3)
CO (ppbv)
Naphthalene
1-Methylnapthalene
2-Methylnaphthalene
Measured
Model
Model (w/ adjusted emissions)
Diurnal Hour (PDT)

Figure SI-4

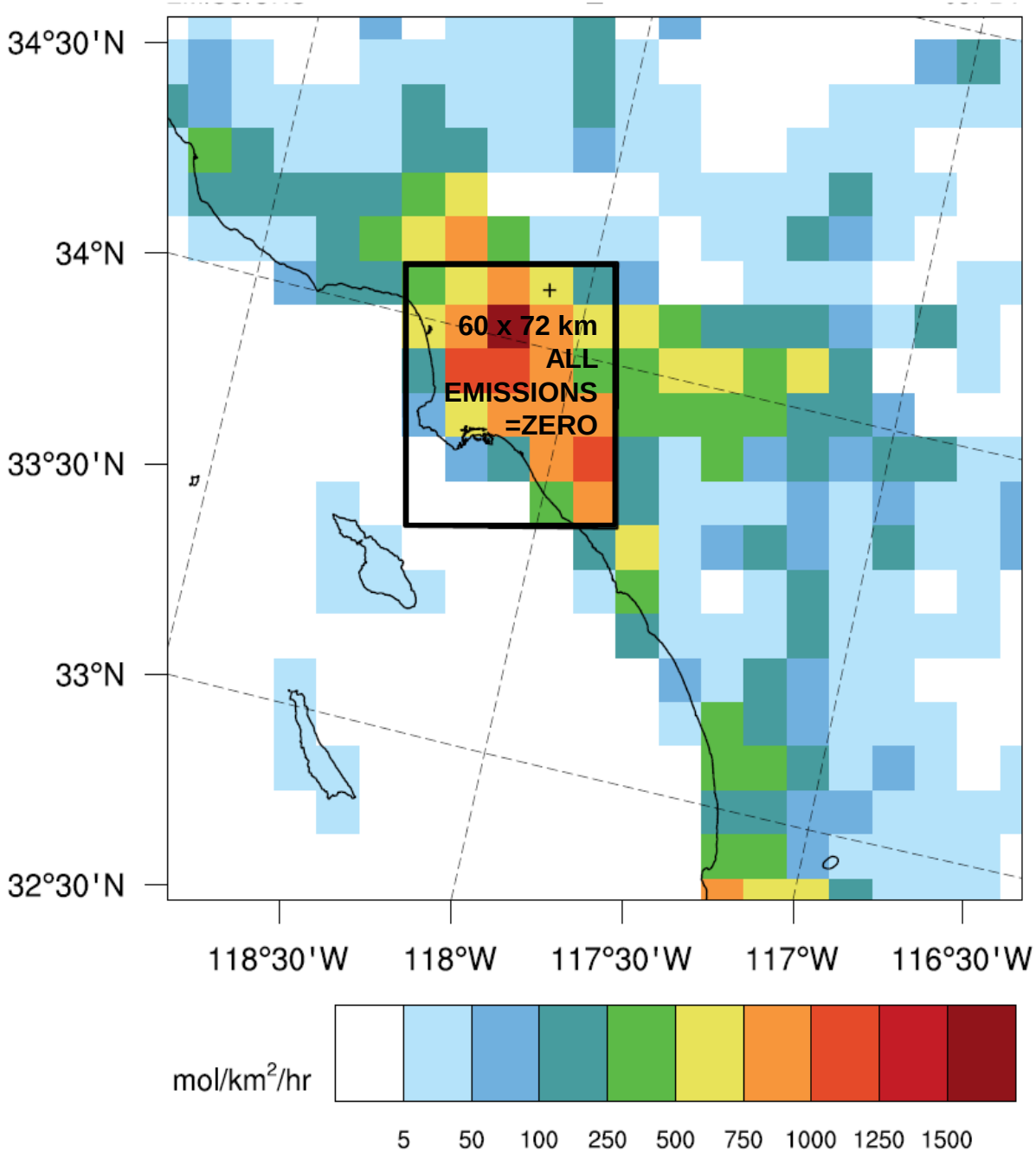
34°30'N
34°N
33°30'N
33°N
32°30'N
118°30'W
118°W
117°30'W
117°W
116°30'W
60 x 72 km
ALL
EMISSIONS
=ZERO
mol/km²/hr
5
50
100
250
500
750
1000
1250
1500

Figure SI-5

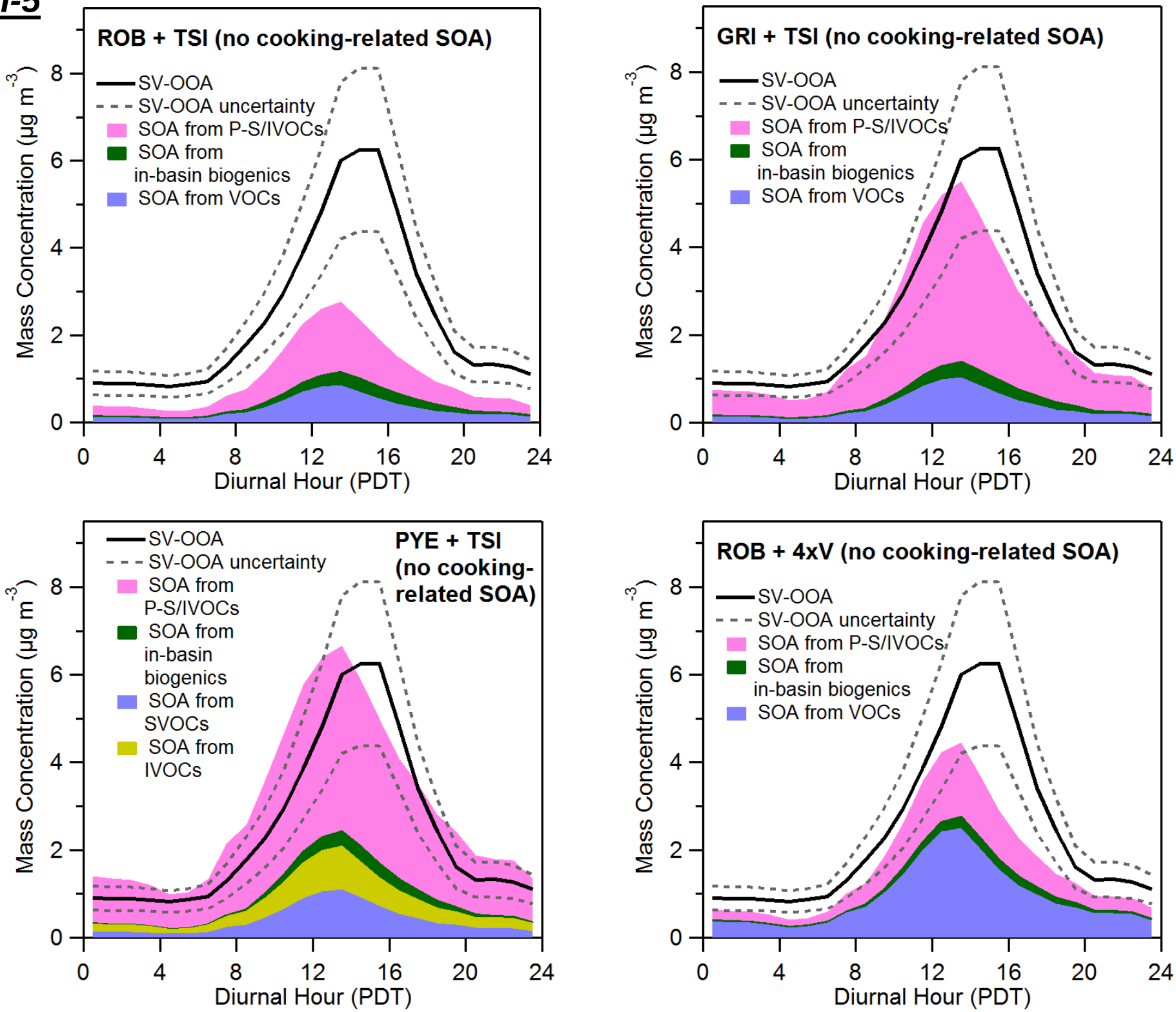
ROB + TSI (no cooking-related SOA)
GRI + TSI (no cooking-related SOA)
PYE + TSI (no cooking-related SOA)
ROB + 4xV (no cooking-related SOA)
SV-OOA
SV-OOA uncertainty
SOA from P-S/IVOCs
SOA from in-basin biogenics
SOA from VOCs
SOA from SVOCs
SOA from IVOCs
Mass Concentration (μg m-3)
Diurnal Hour (PDT)
0
2
4
6
8
0
4
8
12
16
20
24

Figure SI-6

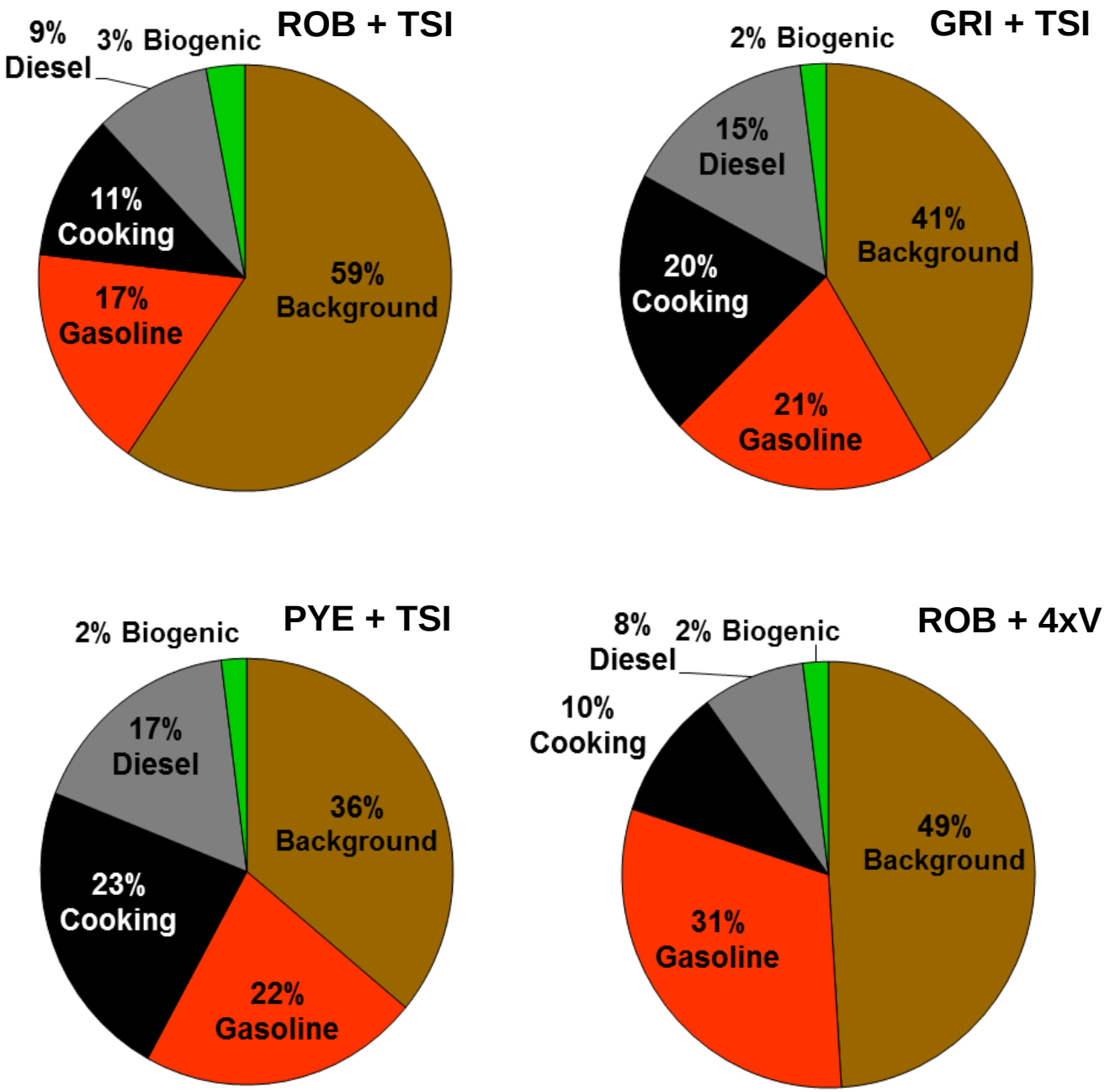
ROB + TSI
9% Diesel
3% Biogenic
11% Cooking
17% Gasoline
59% Background
GRI + TSI
2% Biogenic
15% Diesel
20% Cooking
21% Gasoline
41% Background
PYE + TSI
2% Biogenic
17% Diesel
23% Cooking
22% Gasoline
36% Background
ROB + 4xV
8% Diesel
2% Biogenic
10% Cooking
31% Gasoline
49% Background

Figure SI-7

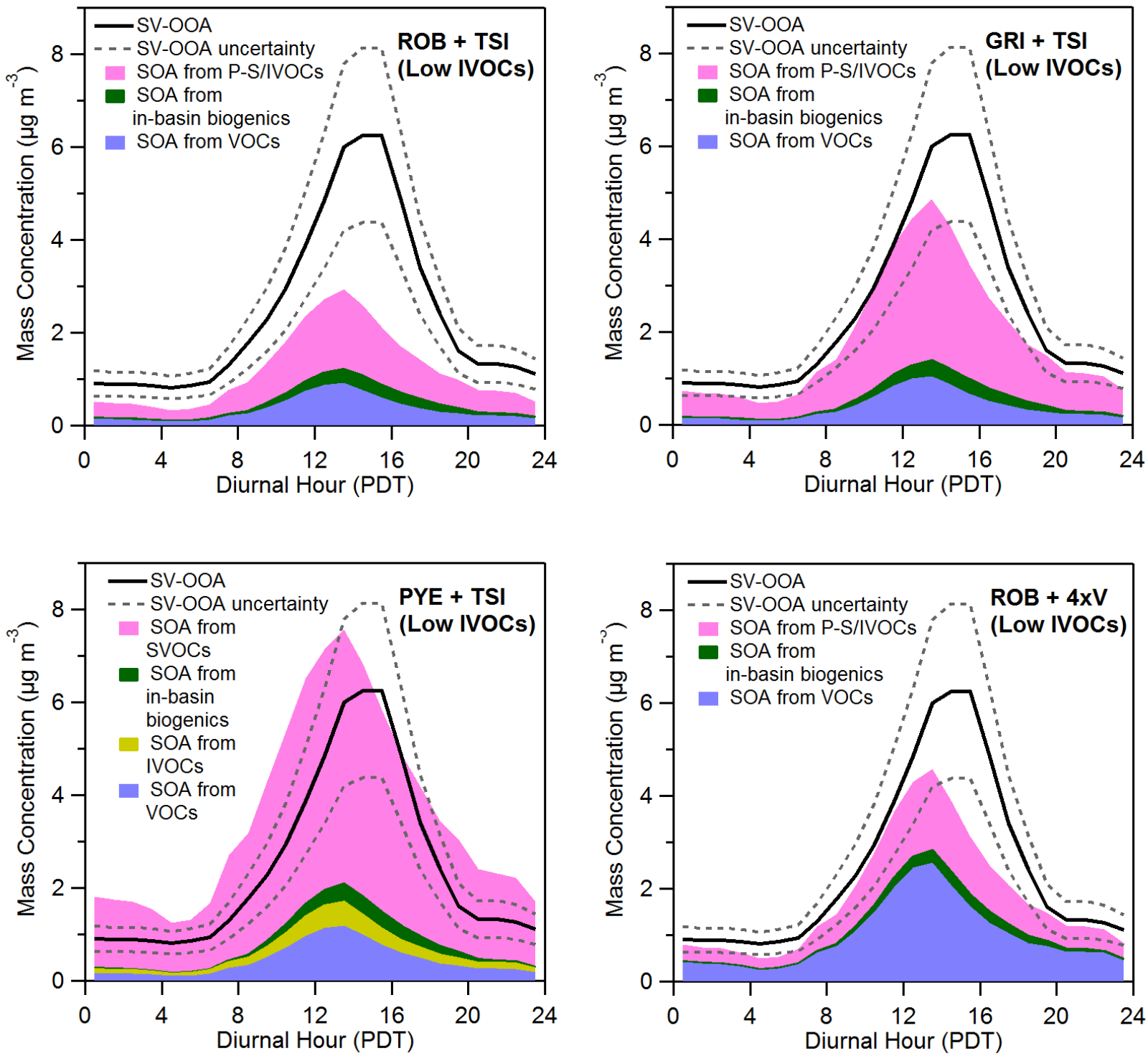
ROB + TSI
(Low IVOCs)
SV-OOA
SV-OOA uncertainty
SOA from P-S/IVOCs
SOA from
in-basin biogenics
SOA from VOCs
GRI + TSI
(Low IVOCs)
PYE + TSI
(Low IVOCs)
SOA from
SVOCs
SOA from
IVOCs
ROB + 4xV
(Low IVOCs)
Mass Concentration (μg m-3)
Diurnal Hour (PDT)
0
2
4
6
8
0
4
8
12
16
20
24

Figure SI-8

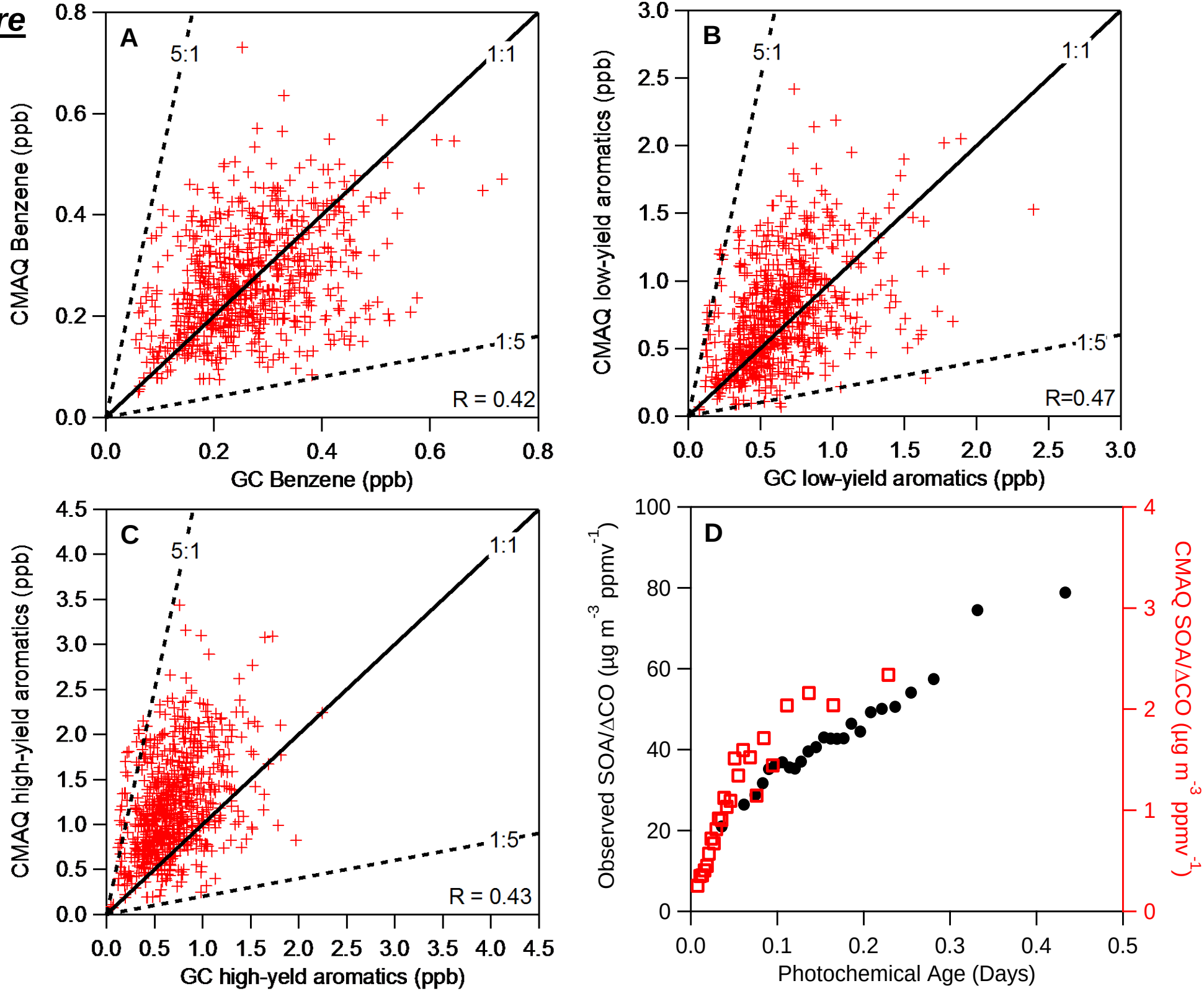
A
5:1
1:1
1:5
R = 0.42
CMAQ Benzene (ppb)
GC Benzene (ppb)
B
5:1
1:1
1:5
R=0.47
CMAQ low-yield aromatics (ppb)
GC low-yield aromatics (ppb)
C
5:1
1:1
1:5
R = 0.43
CMAQ high-yield aromatics (ppb)
GC high-yeld aromatics (ppb)
D
Observed SOA/ΔCO (μg m-3 ppmv-1)
CMAQ SOA/ΔCO (μg m-3 ppmv-1)
Photochemical Age (Days)

Figure SI-9

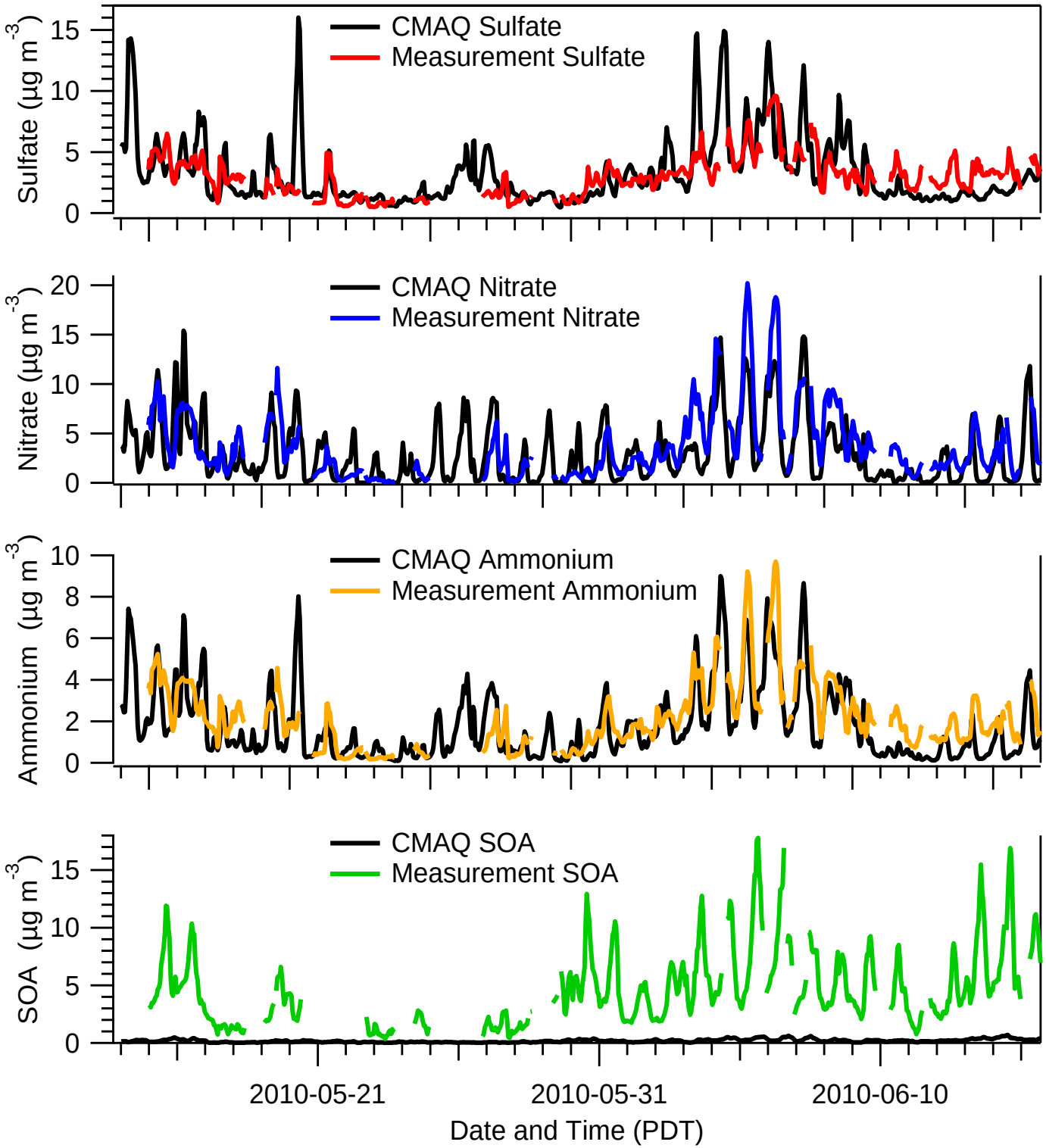
CMAQ Sulfate
Measurement Sulfate
Sulfate (µg m-3)
0
5
10
15
CMAQ Nitrate
Measurement Nitrate
Nitrate (µg m-3)
0
5
10
15
20
CMAQ Ammonium
Measurement Ammonium
Ammonium (µg m-3)
0
2
4
6
8
10
CMAQ SOA
Measurement SOA
SOA (µg m-3)
0
5
10
15
2010-05-21
2010-05-31
2010-06-10
Date and Time (PDT)

Figure SI-10

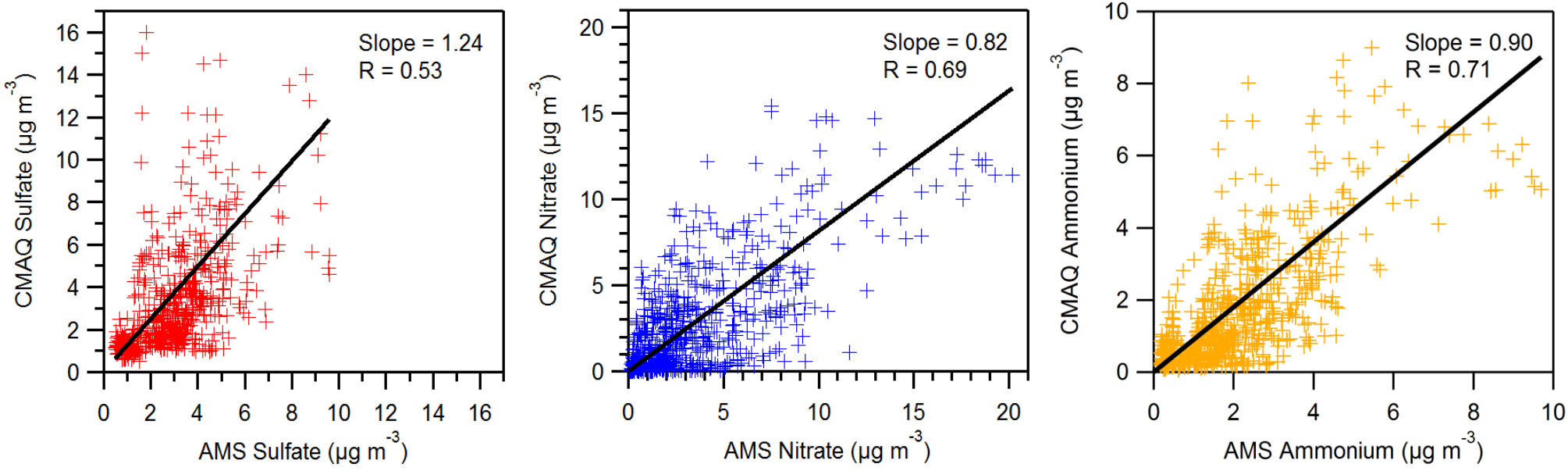
Slope = 1.24
R = 0.53
CMAQ Sulfate (μg m-3)
AMS Sulfate (μg m-3)
Slope = 0.82
R = 0.69
CMAQ Nitrate (μg m-3)
AMS Nitrate (μg m-3)
Slope = 0.90
R = 0.71
CMAQ Ammonium (μg m-3)
AMS Ammonium (μg m-3)